Energy & Environmental Science Accepted Manuscript

Multi-Film Roll Transferring (MRT) Process using Highly Conductive and Solution-Processed Silver Solution for Fully Solution-Processed Polymer Solar Cells

Hongseok Youn,[a] Taehwa Lee,[b] and L. Jay Guo*[ab]

To produce practical large area Polymer solar cells (PSCs), it is highly desirable that the Ag (silver) top electrodes be made by a printing process rather than vacuum evaporation. However, the direct printed electrodes using the highly conductive metal inks such as organometallic and nanoparticle inks, have risks
10 causing the infiltration and contamination of the underlying polymer layers during the printing and annealing processes. Moreover, the metal inks usually require high sintering temperature for the high-conductivity of the electrode. To overcome these limitations, we introduce a multi-layer roll transferring (MRT) approach, in which high performance solution processed Ag electrode is prepared separately from the rest of the organic layers, and the device is completed by a final transferring process. By optimizing the processing conditions of
15 the reductive organometallic Ag solution, the metal electrode has an excellent resistivity (3.4μΩ·cm) and morphology comparable to that of the thermally evaporated silver film. The performances of the devices fabricated by the MRT process were comparable to the metal evaporated devices. Furthermore we achieved fully solution processed devices fabricated by the integration of the roll-to-roll coating of polymer cathode, polymer semiconductor and charge extraction layer and the MRT process.

20 **Broader context**
In the past few years, there were much effort devoted to low-cost polymer solar cells (PSCs) via printing technologies such as roll-to-roll, screen and inkjet printing. The PSCs require highly conductive and reflective metal electrodes for higher efficiency. However, it is hard to directly apply the highly conductive metal inks as the electrode in PSCs because of the penetrating and contamination issues. Here we demonstrate a multi-layer roll transferring (MRT) method instead of the direct printing of metal inks. This method allows a high sintering
25 temperature for the high conductivity of the metal film without the penetrating issues. We achieved the integration of the MRT method with the roll-to-roll process. Similar process can be considered for polymer LED as well.

I. Introduction

Polymer solar cells (PSCs) are considered as a next generation
30 power source due to their light weight, flexibility, low-cost and environmentally friendly manufacturing process.[1-6] These offer fascinating opportunities e.g. for mobile applications as a supplement power source or for the scalable building integrated photovoltaics (BIPV). Moreover, because the functional layers in
35 PSCs can be dissolved in common solvents, they can be manufactured by eco-friendly and scalable printing or coating technologies such as roll-to-roll printing, inkjet printing, screen printing and slot-die coating.[7-10]
Since the introduction of the bulk heterojunction (BHJ) and with
40 the new low band gap polymer material development the power conversion efficiency (PCE) of the polymer BHJ solar cells have now increased to 10%.[11-14]

[a] *Electrical Engineering & Computer Science, The University of Michigan, Ann Arbor, MI, 48109, USA*
[b] *Mechanical Engineering, The University of Michigan, Ann Arbor, MI, 48109, USA. E-mail: guo@umich.edu*

This work will make use of the commonly used poly(3-hexylthiophene):[6,6]-phenyl C_{61} butyric acid methyl ester
45 (P3HT:PCBM) materials, which has reported PCE of $3 - 5\%$.[15-17]

To realize the PSCs as the next generation power source, the manufacturing process needs to be environmentally friendly e.g. employing printing process to minimize the solvent waste, and to
50 use non-halogenated solvent to replace the toxic organic solvents.[18]
Especially a suitable coating or printing process should able to reduce the material cost in large-sized devices because the material cost can be up to 50% (excluding ITO and
55 encapsulation) in PSCs module cost.[19]
The inverted structure in the form of ITO/ZnO/P3HT:PCBM/PEDOT:PSS/Ag is appropriate for the printing process because the top electrode can be replaced with Ag paste and printed by a screen printing or inkjet printing
60 method. The PCE of all-solution processed device via roll-to-roll printing including printed top (back) electrode was reported to be around 1.9% of PCE in inverted structures.[20] However,

This journal is © The Royal Society of Chemistry [year]

Energy Environ. Sci., 2013, **vol**, 00–00 | **1**

because the PEDOT:PSS is an aqueous polymer solution, it is difficult to form good coating on top of the hydrophobic polymer BHJ layer such as P3HT:PCBM. Thus, the PEDOT:PSS solution should be blended with appropriate surfactants and solvents to
5 improve the wetting behaviors on the polymer layer. Moreover, the annealing temperature of the metal inks should be low enough so as not to degrade the organic semiconductors, but the low annealing temperature can significantly impact the conductivity of the metal film. Even though the highly conductive metal inks
10 (organometallic or nanoparticles) have achieved, the residues of reducing agents and organic capping materials or surfactants in the nanoparticle based or organometallic inks are harmful to the underlying polymer layers because they act as impurity contaminant penetrating into the organic semiconductor layer.
15 Therefore, to print the Ag pastes or nanoparticle inks successfully without causing electrical short problems or contamination problems, the underlying PEDOT:PSS layer has to be thick (800nm – 2um) and robust enough to prevent from the potential penetrating problem during the printing and annealing
20 processes.[21]

As an approach to address this problem, the solution processed top metal electrode and the PEDOT:PSS as the hole transport layer can be fabricated separately from the rest of the layer structures. Such an approach is also advantageous in terms of the
25 parallel manufacturing to reduce the processing time. As an example, lamination techniques were reported that two parts which were prepared separately on the flexible substrates contact and bonded each side with high pressure to ensure the conformal contact between the two parts on the hotplate.[22-25] Because the
30 two laminated parts on the two substrates are only sustained by the weak adhesion between the interfaces of the internal films such as PEDOT:PSS and P3HT:PCBM. Thus, the laminated device requires additional adhesion layers against the potential delamination risks.[24,25] In addition, it is hard to achieve the
35 highly conductive and reflective electrodes due to the poor adhesion and aggregation on the polymer substrate using the soluble metal inks, and also they should allow the high processing temperature. Therefore, the metal electrodes were commonly vacuum deposited due to their high reflection or
40 conductivity for the device performances.[22-25]

Therefore, a new fabrication method required to achieve not only the fully solution process but also highly conductive metal electrode using the soluble metal inks.

This paper reports polymer solar cells that are fabricated by full
45 solution-processing steps and proposes a multi-layer roll transferring method as a promising manufacturing process. In this process, the solution processed Ag anode/PEDOT:PSS layers were fabricated separately from the rest of the part where a polymer electrode, a ZnO nanoparticle (NP) based electron
50 transport layer and the P3HT:PCBM active layer were roll-to-roll coated or spin-coated. Importantly, by optimizing the annealing condition, the conductivity of the solution processed Ag film is comparable to the Ag film by the thermal evaporation. The performances of the device fabricated by the multi-film roll
55 transfer technique were comparable to those made by traditional spin-coating and vacuum metal deposition processes.

II. Result and discussion

A. Solution processed highly conductive Ag electrode

60 Among various soluble metal inks, Ag nanoparticle inks and reductive organometallic inks have been widely used due to the high-conductivity.[26-29] e.g. the resistivity of the Ag metal film using the Ag inks has been reported around 6-10μΩ·cm in the literature.[30-33]

65 However, it is hard to directly apply the soluble metal inks as the electrode in PSCs without protection layer because the solution based inks can likely penetrate and contaminate the underlying layers. Therefore, to avoid these issues, the low conductive and less reflective Ag pastes were commonly used in PSCs with a
70 thick PEDOT:PSS layer as the protection layer. However the Ag nanoparticle inks used in the PSCs typically had the resistivity of round 40-100 μΩ·cm[34], and the morphology of the metal film was not smooth due to the aggregation of the ink.[35] These issues lead to the higher series resistance and relatively rough surface in
75 the devices as compared with the devices made by using evaporated metal electrodes, and therefore lower cell efficiency. Here we show that the multi-layer roll transferring method (MRT) can provide efficient way to make device by using the soluble metal solution because the MRT process allows a high
80 processing temperature.

First we introduce the solution processed Ag film as the electrode in PSCs having an excellent conductivity similar to that of the evaporated metal. Specifically, we employing exploit a reductive organometallic Ag precursor solution (Silver 2-
85 ethylhexylcarbamate complex). The purity of the metal and morphology of the reduced metal film are decisive factors for the final film conductivity. To facilitate decomposing of the organic moieties from the organometallic complex, we intentionally increased the reduction time of the Ag precursor, which provides
90 sufficient time to remove the residual organic component. Moreover, a thinner film is used as it can facilitate the evaporation of the decomposed organics molecules from inside the solid film as opposed to that case of the thicker film. As a result, improved conductivity was achieved. Here the film
95 thickness was controlled by adjusting the concentration of the precursor solution and spin-coating speed. In addition, this precursor solution was diluted and homogenized to ensure the film morphology and uniformity. The detailed procedure of the Ag solution preparation was described in the experimental section.
100 The resistivity of the optimized Ag film fabricated by the spin-casting, was only 3.4μΩ·cm, which compare favorably with that of the thermal evaporated Ag film of 2.8 μΩ·cm, as shown in Fig. 1.
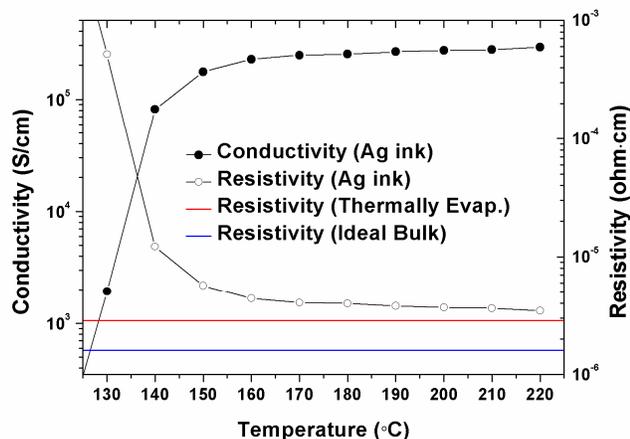
105

110

115

Fig. 1 The conductivity and resistivity of silver film was fabricated by the reductive organometallic Ag solution. The film casted by the spin-coating then soft-baked (90℃) and then sintered at the different temperatures (130-220℃). The thicknesses of the Ag film were measured by the surface profilometer (Dektak) after the sintering process. The resistivity and conductivity were calculated using the parameters of the film thicknesses and sheet resistances (acquired by the 4 point prove measurement tool). The resistivity of the ideal bulk silver is 1.6 μΩ·cm.)

We investigated the reason for achieving such high conductivity in the solution-processed Ag ink film. First, the organic residues or additives in the organometallic complex are decomposed more effectively with increasing annealing temperature, and the Ag organometallic complexes are reduced to very tiny metallic particles (1-2nm). During the sintering process, at lower temperature (under 100℃), the film consists of the disconnected

nanoparticles (<5nm) and therefore is non-conductive. At 100℃ the Ag nanoparticles (10nm) start to merge into larger conductive grains as shown in Fig. 2.
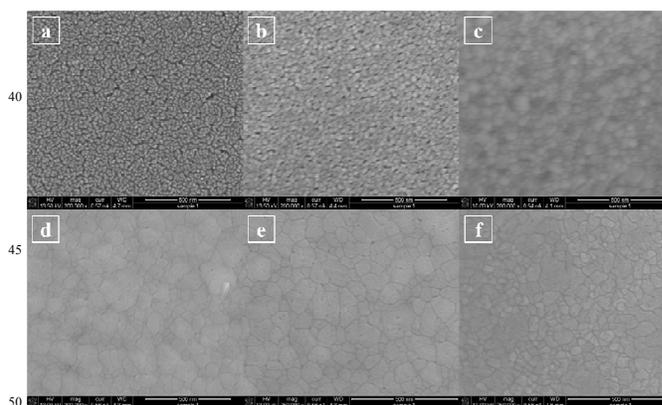

Fig. 2 SEM images of the silver film casted by Ag solution. The Ag nanoparticles were merged and grown into larger grains with respect to the different annealing temperature. (a) 10nm sized nanoparticles were created under the 100℃, (b) merged into 25nm sized nanoparticles networks start to have conductivity under 130℃, (c) 80nm sized grains merged from nanoparticles under 170℃ (d) larger sized 140nm grain was grown under 200℃, (e) 160nm sized grain was grown under 220℃, (f) the surface image of thermal evaporated film for evaluation of the grain size.

We found that higher temperature (>170℃) is required for better conductivity and removal of the residual organic components in the grains. The largest grain size is around 150nm, achieved at 220°C and the corresponding conductivity is the lowest. The morphology of the film using Ag ink is similar to that of the thermally evaporated Ag film. The average roughness of the Ag
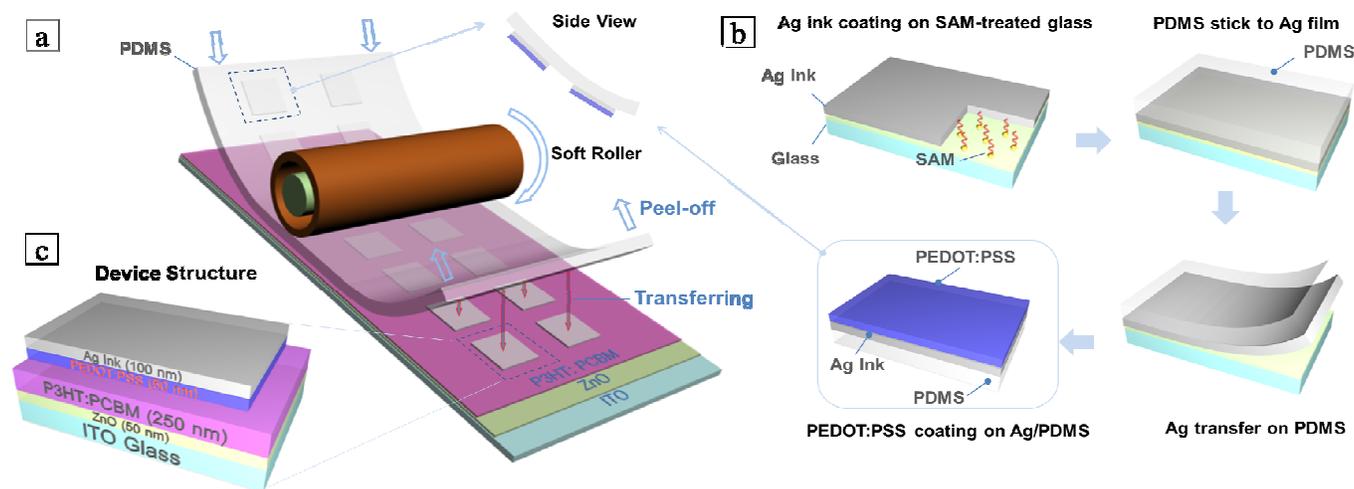

Fig. 3 The illustration of the overall fabrication procedure by the multi-film roll transferring (MRT) method: (a) The highly conductive silver film casted by Ag solution and the PEODT:PSS double layer in the flexible PDMS substrate transferred onto the photo-active layer of P3HT:PCBM with adding mild pressure by using a soft roller. (b) The silver film was coated and annealed on OTS treated glass substrate at 170℃ then the PDMS cover the silver. The silver film transfer to the PDMS and the PEDOT:PSS coated on the back side of silver film. (c) The overall device structure consisting of all-solution processed layers such as ZnO nanoparticle (electron transport layer), P3HT:PCBM (photo-active layer) and PEDOT:PSS/Ag multi-layer by the MRT process.

This journal is © The Royal Society of Chemistry [year]

Energy Environ. Sci., 2013, **vol**, 00–00 | **3**

film of the Ag solution was 1.68nm and thermally evaporated Ag film 1.23nm average roughness. This means that the film casted by the Ag solution is dense enough to have continuous grain network, and its surface quality is good enough as a reflective 5 metal electrode.

B. Transferring process to complete devices

As started earlier, if the Ag ink is applied directly on the organic semiconductor layer, the nanoparticles and organic residues can 10 likely penetrate the polymer layer in the polymer solar cells during the coating and annealing process. To eliminate these contamination issues and allow sufficiently high annealing temperature, we developed a transfer process. We coated the Ag solution onto glass first. After a high-quality conductive film is 15 formed by annealing, it is then transferred to a flexible PDMS layer. As illustrated in Fig. 3(b), the PDMS covers Ag film, which is then gently separated from the substrate without the cracks and deformation of the Ag film. To reduce the adhesion between the Ag film and the glass surface for easy transferring, 20 the glass surface was treated with a self-assembled monolayer (SAM). To do this, OTS (n-octadecyltrichlorosilane) solution was diluted with toluene to 1mM concentration and applied onto the O_2 plasma treated glass. The Ag solution coated on the OTS treated-glass was soft-baked at 135℃ and annealed at 180℃ to 25 produce a highly conductive Ag film.

The Ag film was perfectly transferred to the tacky PDMS substrate, and exhibited a good film quality, which is very critical to the device performance.

The hole transport layer, 50nm thickness of PEDOT:PSS was 30 then coated on top of Ag layer. This stack will be further applied to the polymer active layer during the transferring process.

Parallel to this, a cathode part with stack of films ITO/ZnO/P3HT:PC$_{61}$BM was fabricated separately by spin-coating. A ZnO nanoparticle layer (30nm), for electron transport, 35 and P3HT:PC$_{61}$BM active layer (250nm) was sequentially coated on ITO glass. Lastly, the two separated parts (Ag/PEDOT:PSS and ITO/ZnO/P3HT:PC$_{61}$BM) were attached on the hot plate at 130℃ by the soft roller with a mild pressure [Fig 3(a)]. After removing PDMS, Ag/PEDOT:PSS stack was nicely transferred 40 onto the P3HT:PCBM surface, shown in Fig. 3(c) completing the device fabrication.

The performance of the device fabricated by a multi-layer roll transferring methods (MRT) is comparable to the control devices made by conventional spin-coating of polymer layers and vacuum 45 deposition of the metal anode, although the MRT process was performed in the air. For instance, J-V curves are shown in Fig. 4
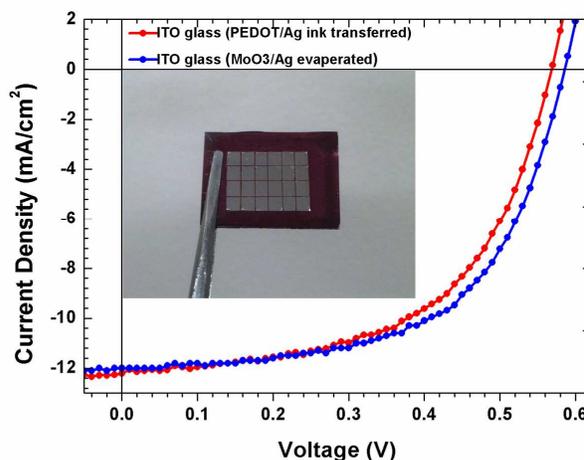

Fig. 4 The J-V device performance of P3HT:PCBM BHJ PSCs according to the device fabrication method such as multi-film roll transferring 65 method (MRT) or simple spin-coating. The blue line represents spin-coated device and the red one represents the device by MRT method. The inner figure in the graph showed the actual device image fabricated by MRT method, the Ag solution and PEODT:PSS were used as reflective anode and hole transport layer respectively.

70

The power conversion efficiency of the MRT device was 3.89%, slightly lower than that of the evaporated device d a decrease in Voc. The key performance parameters including Jsc, Voc, Rs and Rp are summarized in Table 1.

75 To check the relative mechanical adhesion between transferred layers of PEDOT:PSS/Ag and P3HT:PCBM, we attached the adhesive tape and peeled it off from the device as shown in Fig. S1. We could not observe any film delaminated from the devices when the tape was peeled off as shown in Fig. S1(b).

80

C. Roll-to-roll process and ITO-free polymer cathode

As described above, since the spin-coated device exhibited promising performance, the device will be applicable for the roll-to-roll process. Finally we evaluated using the roll coating 85 process to replace the spin-coating to show the scalability of the fabrication process. Moreover, the ITO was replaced by the roll-to-roll compatible polymer cathode.

We first tested coat-ability of the functional layers by the roll-to-roll coating method and the MRT process.

90 In the case of the roll-to-roll process, all layers are coated by a 8" wide roll-to-roll coating systems developed in house, which was controlled by the 400W AC servo-motor and driver as shown in

Table 1 The J-V device performance of P3HT:PCBM BHJ PSCs according to the device fabrication method such as multi-film roll transferring method (MRT), spin-coating and roll-to-roll process.

Roll-to-Roll[a]: Roll-to-roll processed device (PEDOT:PSS cathode, PEIE and P3HT:PCBM layers were roll-to-roll coated in the air atmosphere.)

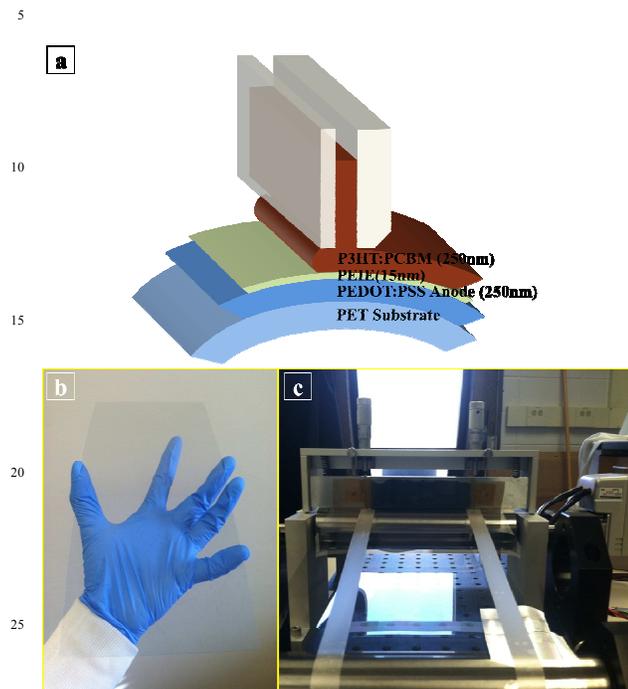|	Jsc (mA/cm^2)	Voc (V)	FF (%)	PCE (%)	Rs (Ω cm^2)	Rp (Ω cm^2)
ITO glass + MoO$_3$/Ag evaporated	12.01	0.59	58.90	4.17	6.64	444
ITO glass + MRT process	12.21	0.58	54.84	3.89	7.21	401
ITO-PET + MoO$_3$/Ag evaporated	11.32	0.57	51.98	3.39	23.43	349
Roll-to-Roll[a] + MRT process	9.52	0.55	57.96	3.04	24.21	443

Fig. 5(c).

Fig. 5 The image of the device structure and designed 8" based roll-to-roll coating system driven by AC servo-motor: (a) Illustration of the device structure and the roll-to-roll coating process via the slit nozzle. (b) The PEDOT:PSS (PH1000 + 5% DMSO) cathode (was roll-to-roll coated on the 6" PET substrate. (c) The image of the roll-to-roll coating process. The various solutions can be contained within the slit inside and the PEDOT:PSS solution is flowing out as creating a wet film when the motor moves.

The coating thickness was mainly controlled by the coating speed. We employed a slit nozzle made of a glass plate and a doctor blade,[36] which contains the coating solutions such as PEDOT:PSS, P3HT:PC$_{61}$BM solution. The solution contained in the slit flows out and creates a meniscus in front of the glass plate, followed by a homogeneous laminar flow at the back of the blade [Fig. 5(a)]. This fine laminar flow is the key to uniformity and film quality.[37] The device structure fabricated by the roll-to-roll coating system is described in the Fig. 5(a).

All layers in the PSCs coated by the roll-to-roll system were processed in the ambient air conditions. First, the PEDOT:PSS (PH1000+5w% DMSO) was coated on PET substrate. We want to point out that PEDOT:PSS was coated, which functions not only as hole transporting layer, but also as a polymer cathode. Two different thicknesses of PEDOT:PSS were tested. The thicker film of the PEDOT:PSS as a polymer electrode has 250nm thickness and 45ohm/sq. sheet resistance. The thick polymer film (250nm) could be achieved by a one-step coating via the blade-slit coating system. The thinner one has 100nm thickness and 110ohm/sq. resistance with a smaller flow rate of the solution. The transmittance of the thicker and thinner polymer electrode was 75.0% and 92.5% respectively. In comparison, the

transmittance of the ITO is 90.0% at the 550nm wavelength as compared in the Fig. 6. Even though the thinner PEDOT:PSS electrode has good transmittance, the sheet resistance is too high, which seriously affects the fill factor of the PV device due to the high series resistance in the device. Therefore, the thicker film was chosen for the efficient device fabricated by roll-to-roll coating.
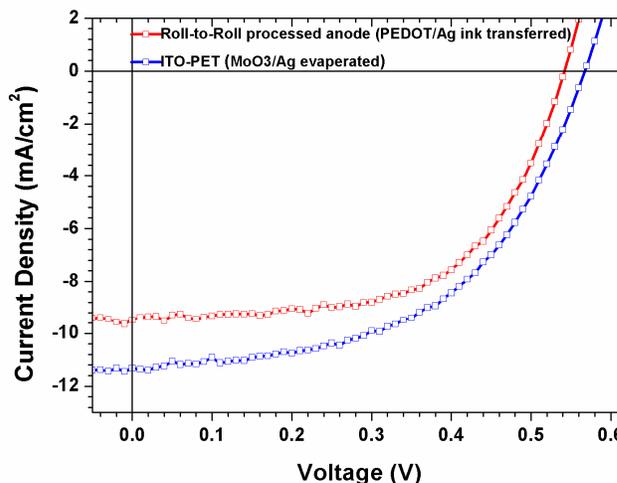

Fig. 6 The transmittances of the transparent electrodes with respect to commercial graded ITO-PET (red), roll-to-roll coated thin polymer electrode (blue) and thick polymer electrode (green). The thickness of the polymer transparent electrode is 100nm and 250nm respectively. The transmittance data was acquired and calibrated via bare PET substrate as a reference substrate.

Next, interfacial layer and photo-active layers were sequentially coated on the anode by the same roll-to-roll coating process. Polyethylenimine (PEI), a work function tuning material by forming interfacial dipole layer, was used that lowers the work function of the PEDOT:PSS electrode.[38]

For the active layer coating (P3HT:PC$_{61}$BM), the solvent in wet coating film was slowly evaporated for creating better crystalline in the ambient air conditions as well known in the literature.[39] The roll-to-roll coating process has the advantage of minimizing the solution waste as compared with the conventional spin-coating process, and therefore more suitable for sustainable and environmentally friendly manufacturing.

For the complete structure, the MRT process again followed. The performance of the device consisting of fully solution processed layers (roll-to-roll processed PEDOT:PSS cathode, PEIE and P3HT:PCBM + anode by solution processed MRT), exhibits a promising power conversion efficiency of 3.04%. The comparison with devices with made on ITO-coated on flexible substrate (PET) and with evaporated Ag anode as is shown in Fig. 7.

Though the PEDOT:PSS layers were used as the cathode and the hole transport layer, Voc was slightly lower than that of the ITO-PET devices with the evaporated MoO$_3$/Ag. The current density of the device using the polymer electrode had 85% of the ITO-PET because the polymer electrode has low transmittance in

This journal is © The Royal Society of Chemistry [year]

Energy Environ. Sci., 2013, **vol**, 00–00 | **5**

whole visual wavelength range as shown in Fig. 6. (The transmittance of the thick polymer electrode at the 550nm wavelength has 83% of the ITO-PET.)

Nevertheless, the maximum power conversion efficiencies of the two devices did not have notable difference due to the higher fill factor than that of ITO-PET. This arises because the surface morphology of the polymer electrodes was very smooth.[36] The smooth surface improves the shunt resistance and thereby increasing fill factor.
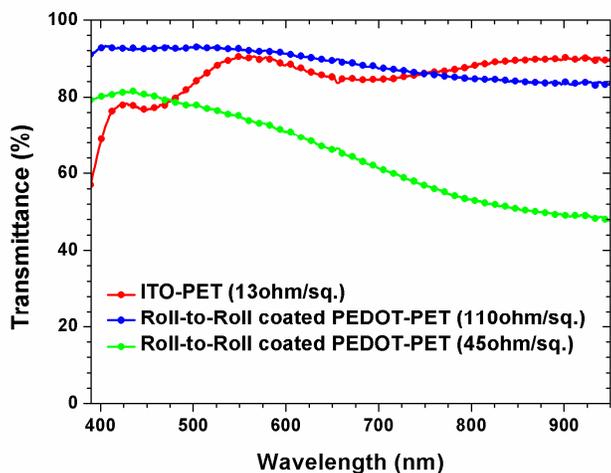

Fig. 7 The J-V device performance of P3HT:PCBM BHJ fabricated by roll-to-roll coated polymer electrode and MRT method. The blue open symbol represents the device fabricated by MRT when using ITO-PET substrate. The red open symbol represents the device fabricated by MRT when using ITO-PET.

III. Conclusion

In conclusion, to achieve the fully solution processed polymer solar cells, we have demonstrated multi-film roll transferring (MRT) process as an effective means to address the difficulty of achieving high conductivity metal electrode by using the Ag inks. The solution processed silver (Ag) film showed exellent conductivity comparable to that of evaporated Ag. Since the Ag film is prepared on the glass substrate modified by the use of SAMs helps to reduce the surface energy, and the transferred Ag film exhibits good film quality without cracks and deformations throughout the MRT process. Compared with direct coating of Ag film on top of the organic layers, the transfer coating of the Ag film is advantageous for preventing potential issues of contamination or attack by solvent udring the printing process.

The solution processed polymer electrode (PEDOT:PSS), interfacial layer and semiconductor polymer blend were coated by using the house-built 8" based roll-to-roll coating system, which allows for full solution process without the waste of the solutions.

We anticipate that the integration of the MRT method with roll-to-roll process can be developed as a practical approach for large area manufacturing of organic photovoltaics.

IV. Experimental

A. Polymer PV cells fabrication on the ITO-glass substrate

Control device of the PSCs have the following structure: ITO-glass/ZnO nanoparticle layer/P3HT:PCBM/MoO$_3$/Ag. ITO-glass was cleaned with acetone and isopropyl alcohol sequentially in the ultrasonic bath. ZnO nanoparticles were synthesized and dispersed into butanol as described elsewhere.[40] ZnO nanopaticle solution was spin-coated on the precleaned ITO-glass substrate at 3000rpm. After the baking on the hotplate, the thickness of the film was 30nm. P3HT:PCBM solution blended with 1:0.8 ratio in the dicholorobenzne was spin-coated on the ZnO nanoparticle layer at 1000rpm spin-rate. P3HT:PCBM layer was kept and dried for creation of the crystalline of the 200nm-250nm BHJ film for 20min. MoO$_3$(10nm) and Ag(100nm) layers were thermal evaporated in the vacuum chamber under 10^{-6} bar. All fabication steps processed in the nitrogen filled glob-box environment.

The MRT processed devices were fabricated the same with the control device except the solution processed PEDOT:PSS/Ag film. All the film thicknesses were acquired and analyzed from Dektak Surface Profilometer or SEM. The device performances were measured by Keithley 2400 sroce-meter system synchronized with the illuminating the polymer solar cells using Oriel solar simulator (xenon lamp and AM 1.5 G filter) at the irradiation intensity of 100 mW cm^{-2}, calibrated by NREL-certified Si reference cell. All measurements of the PSCs were performed under ambient air conditions.

B. Roll-to-roll coating process on the flexible substrate

Roll-to-roll processed and MRT processed devices ware produced by following process. As the flexible substrate, 6" and 120um PET was surface-treated by O$_2$ plasma at 100W for 30sec. The PEDOT:PSS (PH1000 + 5w% DMSO) solution was injected into blade-slit space and then coated on the PET substrate. The film thickness of PEDOT:PSS electrode having a different conductivity was controlled by adjusting the coating speed from 10 to 20mm/sec. The blade-gab from the substrate was controlled 50um-100um according to the layers. Other layers, such as PEIE (0.4w% into 2-methoxyethanol) and P3HT:PCBM were roll-to-roll coated. The blade gap between the blade and the substrate was fixed with 50um. The solution processed and patterned 1cm^2 (active area) Ag and PEDOT:PSS layer was transferred on the roll-to-roll processed P3HT:PCBM layer.

C. Ag soultion process and MRT process

The 10w% Ag solution (silver 2-ethylhexylcarbamate complex, provided by Inktec Inc.) of the reductive type was diluted by isopropanol with 20-50v% precursor concentrations. Typically the film from 50v% has 150nm thickness. The diluted and mixed Ag solution was homogenized in the ultrasonic bath. The Ag solution was coated on the n-octadecyltrichlorosilane (OTS) deposited glass substrate. The glass was treated by O$_2$ plasma at 200W for 60sec and the subject to the OTS solution (1mM at toluene) for 30min. Finally, the substrate was washed by the toluene and water sequentially in the ultrasonic bath.

For MRT process, 2mm thick PDMS (Sylgard 184, Dow Corning

6 | *Energy Environ. Sci.*, 2013, **vol**, 00–00

This journal is © The Royal Society of Chemistry [year]

Corp.) substrate was wrapped on the surface of the Ag film. After the Ag film was transferred on the PDMS, the surface was UV ozone ramp treated and coated with the PEDOT:PSS (Clevios PV P AI4083) as hole transport layer. During the MRT process, a soft rubber roller was used for adding a mild pressure and annealing at 130℃.

References

1 N. Espinosa, M. Hösel, D. Angmo and F. C. Krebs, *Energy Environ. Sci.*, 2012, **5**, 5117.

2 C. R. McNeill, Energy Environ. Sci., 2012, **5**, 5653.

3 W. Chen, M. P. Nikiforov and S. B. Darling, *Energy Environ. Sci.*, 2012, **5**, 8045.

4 H. Ma, H.-L. Yip, F. Huang and A. K.-Y. Jen, *Adv. Funct. Mater.*, 2010, **20**, 1371.

5 B. P. Lyons, N. Clarke and C. Groves, *Energy Environ. Sci.*, 2012, **5**, 7657.

6 J. D. Servaites, M. A. Ratner and T. J. Marks, *Energy Environ. Sci.*, 2011, **4**, 4410.

7 F. C Krebs, S. A. Gevorgyan and J. Alstrup, *J. Mater. Chem.*, 2009, **19**, 5442.

8 H. J. Park, M.-G. Kang, S. H. Ahn and L. J. Guo, *Adv. Mater.*, 2010, **22**, E247.

9 F. C. Krebs, T. Tromholt and M. Jørgensen, *Nanoscale,* 2010, **2**, 873.

10 Y. Galagan, J.-E. J. M. Rubingh, R. Andriessen, C.-C. Fan, P. W. M. Blom, S. C. Veenstra, J. M. Kroon, *Sol. Energy Mater. Sol. Cells,* 2011, **95**, 1339.

11 Z. He, C. Zhong, X. Huang, W.-Y. Wong, H. Wu, L. Chen, S. Su and Y. Cao, *Adv. Mater.*, 2011, **23**, 4636.

12 H.-Y. Chen, J. Hou, S. Zhang, Y. Liang, G. Yang, Y. Yang, L. Yu, Y. Wu and G. Li, *Nat. Photon.*, 2009, 3, 649.

13 C. E. Small, S. Chen, J. Subbiah, C. M. Amb, S.-W. Tsang, T.-H. Lai, J. R. Reynolds and F. So, *Nat. Photon.*, 2012, **6**, 115.

14 Z. He, C. Zhong, S. Su, M. Xu, H. Wu and Y. Cao, *Nat. Photon.*, 2012, **6**, 591.

15 H. J. Park, H. Kim, J. Y. Lee, T. Lee and L. J. Guo, *Energy Environ. Sci.*, 2013, **6**, 2203.

16 M. T. Dang, L. Hirsch and G. Wantz, Adv Mater., 2011, 23, 3597.

17 S. K. Hau, H.-L. Yip, O. Acton, N. S. Baek, H. Ma and A. K.-Y. Jen, *J. Mater. Chem.*, 2008, **18**, 5113.

18 C.-C. Chueh, K. Yao, H.-L. Yip, C.-Y. Chang, Y-X. Xu, K.-S. Chen, C.-Z. Li, P. Liu, F. Huang, Y. Chen, W.-C. Chenb and A. K.-Y. Jen, *Energy Environ. Sci.*, 2013, **6**, 3241.

19 Serge Beaupre and Mario Leclerc, *J. Mater. Chem. A*, 2013, **1**, 11097.

20 J.-S. Yu, I. Kim, J.-S. Kim, J. Jo, T. T. Larsen-Olsen, R. R. Søndergaard, M. Hösel, D. Angmo, M. Jørgensen and F. C. Krebs, *Nanoscale*, 2012, **4**, 6032.

21 D. Angmo , J. Sweelssen , R. Andriessen , Y. Galagan and F. C. Krebs, *Adv. Energy Mater.,* 2013, **3**, 1230.

22 M. Nakamur, C. Yang, E. Zhou, K. Tajima and K. Hashimoto, *ACS Appl. Mater. Interfaces*, 2009, **12**, 2703.

23 D. Gupta , M. M. Wienk and R. A. J. Janssen, *Adv. Energy Mater.,* 2013, **3**, 782.

24 Y. Lu, C. Alexander, Z. Xiao, Y. Yuan, R. Zhang and J. Huang, *Nanotechnology*, 2012, **23**, 344007.

25 D. Kaduwal, B. Zimmermann, U. Würfel, *Sol. Energy Mater. Sol. Cells,* 2014, **120**, 449.

26 K. Ankireddy, S. Vunnam, J. Kellara and W. Cross, *J. Mater. Chem. C*, 2013, **1**, 572.

27 Y. Li, Y. Wu and B. S. Ong, *J. Am. Chem. Soc.*, 2005, **127**, 3266.

28 Y.-L. Tai and Z.-G. Yang, *J. Mater. Chem.*, 2011, **21**, 5938.

29 J. Perelaer, C. E. Hendriks, A. W. M. Laat and U. S. Schubert, *Nanotechnology*, 2009, **20**, 165303.

30 B. Y. Ahn, D. J. Loranga and J. A. Lewis, *Nanoscale*, 2011, **3**, 2700.

31 Y.-L. Tai and Z.-G. Yang, *J. Mater. Chem.*, 2011, **21**, 5938.

32 Y. Tao, Y. Tao, B. Wang, L. Wang and Y. Tai, *Nanosclae. Res. Lett.*, 2013, **8**, 296.

33 Y. Wu, Y. Li and B. S. Ong, *J. Am. Chem. Soc.*, 2007, **129**, 1862.

34 C. Girotto, B. P. Randa, S. Steudel, J. Genoea, P. Heremans, *Org. Electon.*, 2009, **10**, 735.

35 S. K. Haua, H.-L. Yip, K. Leong, A. K.-Y. Jen, *Org. Electon.*, 2009, **10**, 719.

36 S. Shin, M. Yang, L. J. Guo, H. Youn, *Small*, 2007, **9**, 4036.

37 H.S. Youn, H.S. Kim and L. Jay Guo, "Low-Cost Fabrication of Organic Photovoltaics and Polymer LEDs", in "Low-cost Nanomaterials: Toward Greener and More Efficient Energy Applications", edited by Z. Lin and J. Wang, Springer

38 Y. Zhou, C. F.-Hernandez, J. Shim, J. Meyer, A. J. Giordano, H. Li, P. Winget, T. Papadopoulos, H. Cheun, J. Kim, M. Fenoll, A. Dindar, W. Haske, E. Najafabadi, T. M. Khan, H. Sojoudi, S. Barlow, S. Graham, J.-L. Brédas, S. R. Marder, A. Kahn, B. Kippelen, Science, 2012, **336**, 327.

39 G. Li, V. Shrotriya, J. Huang, Y. Yao, T. Moriarty, K. Emery and Y. Yang, *Nat Mater.*, 2005, **4**, 864.

40 W.J.E. Beek, M.M. Wienk, M. Kemerink, X. Yang and R.A.J. Janssen, *J. Phys.Chem. B*, 2005, **109**, 9505.